Global Change Biology

Global Change Biology (2013) **19**, 1720–1735, doi: 10.1111/gcb.12173

Implications of nonrandom seed abscission and global stilling for migration of wind-dispersed plant species

SALLY E. THOMPSON* and GABRIEL G. KATUL†

*Department of Civil and Environmental Engineering, University of California, Berkeley, California 94710, USA, †Nicholas School of the Environment, Levine Science Research Center, Duke University, Durham, NC27708-0328, USA

Abstract

Migration of plant populations is a potential survival response to climate change that depends critically on seed dispersal. Biological and physical factors determine dispersal and migration of wind-dispersed species. Recent field and wind tunnel studies demonstrate biological adaptations that bias seed release toward conditions of higher wind velocity, promoting longer dispersal distances and faster migration. However, another suite of international studies also recently highlighted a global decrease in near-surface wind speeds, or 'global stilling'. This study assessed the implications of both factors on potential plant population migration rates, using a mechanistic modeling framework. Nonrandom abscission was investigated using models of three seed release mechanisms: (i) a simple drag model; (ii) a seed deflection model; and (iii) a 'wear and tear' model. The models generated a single functional relationship between the frequency of seed release and statistics of the near-surface wind environment, independent of the abscission mechanism. An Inertial-Particle, Coupled Eulerian-Lagrangian Closure model (IP-CELC) was used to investigate abscission effects on seed dispersal kernels and plant population migration rates under contemporary and potential future wind conditions (based on reported global stilling trends). The results confirm that nonrandom seed abscission increased dispersal distances, particularly for light seeds. The increases were mitigated by two physical feedbacks: (i) although nonrandom abscission increased the initial acceleration of seeds from rest, the sensitivity of the seed dispersal to this initial condition declined as the wind speed increased; and (ii) while nonrandom abscission increased the mean dispersal length, it reduced the kurtosis of seasonal dispersal kernels, and thus the chance of long-distance dispersal. Wind stilling greatly reduced the modeled migration rates under biased seed release conditions. Thus, species that require high wind velocities for seed abscission could experience threshold-like reductions in dispersal and migration potential if near-surface wind speeds continue to decline.

Keywords: anemochory, global stilling, Lagrangian modeling, seed dispersal, seed abscission

Received 30 August 2012; revised version received 6 January 2013 and accepted 29 January 2013

Introduction

The potential speed at which plant populations can migrate is an important determinant of the likely impact of climate change on species distributions and biodiversity (Loarie *et al.*, 2009). When plant populations have a suitable environment available to colonize, their maximum migration rate becomes strongly determined by seed dispersal (Clark, 1998; Higgins & Richardson, 1999; Clark *et al.*, 2001; Thompson & Katul, 2008). The transport of wind-dispersed seeds can be described using physical models (Okubo & Levin, 1989; Tackenberg, 2003; Kuparinen *et al.*, 2007; Nathan *et al.*, 2011b) that aim to predict the seed dispersal kernel, which is the probability density function of seed travel distances from the parent source. The moments of the dispersal kernel determine important ecological and evolutionary outcomes for plants (Portnoy & Willson, 1993). As examples, the mean dispersal distance is related to seedling survival and recruitment, especially in situations where predation decreases with distance from the parent (Hubbell, 1980; Thompson *et al.*, 2009, 2010). In addition, high kurtosis in the kernel indicates a high probability of long-distance travel events, and is connected to rapid rates of migration (Clark, 1998; Higgins & Richardson, 1999; Clark *et al.*, 2001; Thompson & Katul, 2008).

The form of the seed dispersal kernel is determined by a combination of biological and physical factors, including the (i) mass and release height of seeds; (ii) leaf area distribution in the plant canopy; and (iii) prevailing wind conditions during dispersal (Katul *et al.*, 2005; Nathan & Katul, 2005; Jongejans *et al.*, 2007). While most predictions of maximum migration rate and seed dispersal assume that these factors are unchanging, recent studies highlight that most observed mean near-surface wind speeds have declined in the past 30–50 years (McVicar *et al.*, 2008; Guo *et al.*, 2011; McVicar *et al.*, 2012b). This decline has been attributed

Correspondence: Sally E. Thompson, tel. +1 510 642 1980, fax +1 510 643 5264, e-mail: sally.thompson@berkeley.edu

to increased surface roughness due to vegetation growth, afforestation, or urbanization (McVicar *et al*., 2008; McVicar & Roderick, 2010; Vautard *et al*., 2010), suppression of the East Asian monsoon (Xu et al. 2006), and the warming effect of aerosols on the upper atmosphere (McVicar & Roderick, 2010; Vautard *et al*., 2010). The mean global trend in wind speed over the past 30 years has been estimated as -0.014 $ms^{-1}a^{-1}$, or a $\approx$15% decline, based on regional studies with at least 30 site observations over at least 30 years (Roderick *et al*., 2007; McVicar *et al*., 2012b). This global stilling trend is widespread in the Northern Hemisphere (Vautard *et al*., 2010; McVicar *et al*., 2012b), where wind-dispersed plants are common, and the implications on plant migration are a recognized ecological outcome of slowing near surface wind speeds that requires investigation (McVicar et al. 2012a). Effects on migration may be particularly marked in plants that only release seeds for dispersal during high wind speed conditions (Wright *et al*., 2008). Such nonrandom abscission is now reported in field studies (Greene & Johnson, 1992; Maurer *et al*., 2013) and wind tunnel experiments (Jongejans *et al*., 2007; Soons & Bullock, 2008; Greene & Quesada, 2011). Bias in seed release arises as a consequence of adaptive strategies that alter the geometry and material structure of links between plants and seeds (Pazos *et al*., 2013). By biasing seed release toward higher wind speeds, plants could hypothetically increase their dispersal length scales and migration rates under ambient wind conditions (Greene & Johnson, 1992; Greene, 2005; Skarpaas *et al*., 2006; Bohrer *et al*., 2008; Soons & Bullock, 2008; Greene & Quesada, 2011). In the context of an observed decline in wind speeds, however, seed releases that are biased toward high wind speeds could be disproportionately reduced, potentially resulting in a nonlinear, or threshold-like, decline in dispersal and migration of these species under continued global stilling scenarios.

This study examines the sensitivity of maximum predicted plant population migration rates of wind-dispersed species to reductions in near-surface wind speed and bias in seed release conditions. First, we examine the potential modes of nonrandom seed abscission. Researchers have identified a range of empirical patterns of abscission behavior (Jongejans *et al*., 2007; Soons & Bullock, 2008; Greene & Quesada, 2011), while modeling studies have tended to prescribe sigmoidal or threshold dependencies of seed release on ambient wind speed (Greene & Johnson, 1992; Schippers & Jongejans, 2005; Bohrer *et al*., 2008; Pazos *et al*. 2013). We investigate the genesis of these different patterns and the justification for a particular choice of abscission probability function by developing three contrasting physical models of seed abscission and subjecting them to different patterns of mean wind speed variation. Second, the seed release results are generalized and combined with a Coupled Eulerian-Lagrangian Closure (CELC) model (Nathan & Katul, 2005; Poggi *et al*., 2006), modified here to account for inertial particles (IP-CELC), to explore the sensitivity of seed trajectories and dispersal kernels to nonrandom abscission. The novelties of the IP-CELC approach include accounting for the following: (i) multiple timescales of variability in the wind-field; (ii) the effects of a plant canopy on wind (critical for wind-dispersed tree species); and (iii) the effects of seed inertia, or imperfect coupling between wind and seed velocities. This mechanistic framework is essential to explore the effects of initial conditions of seed and wind velocity, as well as vertical variation in the wind statistics, on the dispersal kernel. These factors are not addressed by simpler analytical models (Katul *et al*., 2005). Third, to address the role of stilling, predicted changes in mean hourly wind speed are converted to predicted changes in the probability density function (pdf) of hourly mean wind speeds, assuming that the pdf can be described with a conventional Weibull probability law (Thompson *et al*., 2008). The joint effects of stilling and nonrandom abscission are then investigated by combining the kernels generated from IP-CELC with the projected stilled wind speed pdfs. We consider the end-member cases of perfect and spherical coupling between the wind and the seed velocities, and the sensitivity of the results to different mean canopy heights and seed terminal velocities. The resulting kernels from these simulations are fitted with an analytical dispersal model (the WALD Model) (Katul *et al*., 2005). The parameters of WALD can be related to maximum potential population migration rates as shown elsewhere (Thompson & Katul, 2008), allowing an exploration of the sensitivities of stilling and nonrandom seed release on maximum migration rates. Finally, the potential ecological consequences of an interaction between stilling and abscission dynamics on the composition of migrating forest assemblages are illustrated with a synthetic example. A schematic diagram is presented in Fig. 1, illustrating the connections between the different models and processes.

Materials and methods

The development of the models for abscission, the modification to generate IP-CELC, and their implementation are described here. Further theoretical details, including specifics of the abscission models, the unmodified CELC and WALD models, and details of the wind and canopy datasets, are provided as Supporting Information. The methods section starts

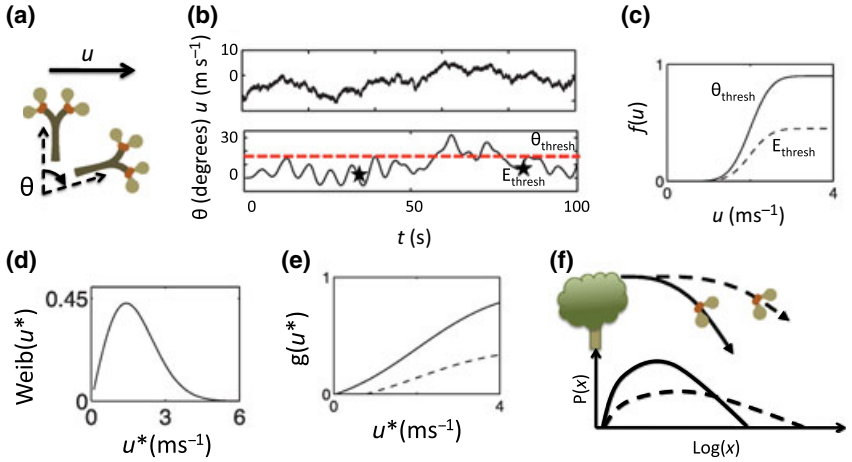

Fig. 1. Conceptual model illustrating the progression from release mechanism to dispersal kernel, via the fluctuations in u and u^*. Panel a illustrates seeds swaying on a tree. Panel b relates the fluctuations in the wind speed u to the stem angle, θ. Oscillations in θ will lead to different abscission behavior under a threshold angle model (θ_{thresh} is shown as a dashed line) and an accumulated energy model (starred locations). The models result in different probabilities of abscission, $f(u)$, given the instantaneous wind speed (Panel c), or the hourly shear velocity ($g(u^*)$, Panel e). When combined with the seasonal distribution of the shear velocity (Panel d), and hourly dispersal kernels generated from IP-CELC, the seasonal dispersal kernels can be predicted given different release scenarios (Panel f).

with a discussion of how different timescales of fluctuation in wind speed influences seed abscission, seed dispersal and thus migration rates, because these relationships underpin all subsequent analyses.

Timescales of fluctuations in wind speed and their implications

Abscission influences seed dispersal in two ways, on widely separated timescales: (i) by biasing the initial wind velocity experienced by the seed at the time of release (Greene, 2005); and (ii) by changing the wind environment experienced by the population of dispersing seeds. To elaborate on this point, variation in the wind speed on different timescales must be distinguished. The fastest variations in the wind speed (on the order of seconds) are turbulent fluctuations around the hourly mean wind speed (Nathan *et al.*, 2011b), illustrated in Panel b, Fig. 1, and designated by u' [ms^{-1}]. These fluctuations determine the instantaneous velocity that creates drag and provides the energy for seed abscission. Turbulent fluctuations inside canopies are coherent on timescales of around 1–10 s (Katul *et al.*, 1997). The fluctuations persist long enough to lift mobile seeds above the canopy, exposing them to the elevated mean wind speeds prevailing above the canopy (Nathan *et al.*, 2002; Katul *et al.*, 2005). Turbulent fluctuations therefore increase dispersal length scales and potential migration rates, and must be accounted for when considering abscission and dispersal (Clark *et al.*, 1998; Clark, 1998; Nathan *et al.*, 2011b). The second timescale is set by variation in the mean horizontal wind velocity $\overline{u}$ [ms^{-1}], where the over-bar denotes hourly time averaging. This velocity is often statistically steady on timescales of 0.5–1 h (Van der Hoven, 1957), so individual seeds experience a single mean wind speed during dispersal. A population of seeds, however, disperses over a period of days to months, during which time the hourly mean wind speeds fluctuate. These fluctuations often follow a Weibull probability distribution (Panel d in Fig. 1). The Weibull fluctuations in hourly mean wind speed interact with turbulent variations to increase dispersal distances and migration rates (Thompson & Katul, 2008). Nonrandom abscission increases the instantaneous (turbulent) wind velocity at release, biasing the initial conditions of the seed and potentially the remainder of its trajectory. At seasonal timescales, nonrandom abscission skews the distribution of hourly wind speeds experienced by the dispersing seeds, compared to the ambient Weibull distribution (Pazos *et al.*, 2013). Of course, long-term phenomena such as global stilling may change the parameters of the Weibull distribution itself.

Above uniformly distributed vegetated canopies, flow properties such as the hourly mean wind speed vary with elevation z [m] [e.g. (Prandtl, 1904)]. A conveniently height-independent metric of the wind properties is provided by the shear or friction velocity (u^* [ms^{-1}]) above the canopy. The u^* measures the kinematic turbulent shear stress at the top of the canopy. Numerous canopy experiments show that the wind statistics scale with u^* (Raupach & Thom, 1981; Finnigan, 2000) for nonstratified atmospheric flows. Variability of the wind speed and its statistics can thus be determined from u^*. For example, when the hourly variations in $\overline{u}$ follow a Weibull distribution, u^* generally follows a similar probability law (see Fig. 2).

Seed abscission mechanisms

Abscission is the separation of a seed from its attachment to the parent plant. Modeling the effects of nonrandom seed abscission requires relating the abscission probability to

instantaneous wind conditions, and ultimately the wind statistics. Several authors have proposed sigmoidal or threshold functional relationships between abscission probability and instantaneous wind speeds (Greene & Johnson, 1992; Schippers & Jongejans, 2005; Bohrer *et al*., 2008; Pazos *et al*., 2013). Here, the aim was to investigate the theoretical basis for such assumptions. Three hypotheses for the separation mechanism are considered. First, the drag force exerted on the seed by the wind could exceed the tensile strength of the connective tissue, causing it to break. The tensile strength could be fixed (Hypothesis 1), or might decline as wind causes the seed to move back and forth (Panel a, Fig. 1). The decline in tensile strength should scale with the absorption of angular kinetic energy (from the shaking seed) by the connective tissue (Hypothesis 2). A third mechanism (Hypothesis 3) assumes that seeds are held in rigid pods or cones that expose seed for dispersal once tilted beyond some threshold. These hypotheses focus on localized wind-seed interactions, and variations in temperature, humidity, and seed maturity that also affect abscission require separate consideration (Greene & Johnson, 1992; Skarpaas *et al*., 2006). To account for angular motion of seeds (required for the wear and tear and threshold angle hypotheses), a simplified numerical model of wind-forced plant motion was used (de Langre, 2008) and is fully described in the Supplementary Material. If tensile strength is fixed, however, then abscission probabilities can be analytically determined from the statistics of the wind.

Fixed tensile strength: the simple rupture model. In this model, abscission occurs if the instantaneous drag force D, [N] on a seed exceeds the tensile strength of the seed-plant connection. The drag (D) exerted on an object in turbulent flow is given by (Batchelor, 1967):

$$D = \frac{C_D \rho A_S u^2}{2}, \tag{1}$$

where C_D is the dimensionless drag coefficient (≈ 0.4), ρ,[kg m^{-3}] is the fluid density, A_s, [m^2] the surface area intercepting the flow, and u, [ms^{-1}] the instantaneous wind speed.

The abscission probability $p(abs)$ is zero provided u is less than the threshold velocity at which D causes rupture, denoted u_{thresh}. For $u \geq u_{thresh}$, $p(abs) = 1$. For a steady mean wind speed $\overline{u}$ and neutral atmospheric conditions, u has a near-Gaussian distribution with variance σ_u^2 (Chu *et al*., 1996). The frequency of abscission $f(u)$ (Panel c, Fig. 1) on hourly timescales is approximated from the cumulative density function of u:

$$f(u) = \int_{u_{thresh}}^{\infty} \frac{1}{\sigma_u \sqrt{2\pi}} e^{\frac{-(u-\overline{u})^2}{2\sigma_u}} du. \tag{2}$$

The D needed for rupture may be estimated from the tensile strength of plant tissue: For example, 0.1–5 Nmm^{-2} for nonlignified, desiccated tissue (Hedderson *et al*., 2009). Scanning electron microscope images of dandelion pappi suggest their surface area A_s is ≈ 2.2 cm^2; and the point of contact between diaspore and plant around 50–100 μm (Sudo *et al*., 2008). Terminal velocity data indicate that $C_D \approx 0.4$ (Sudo *et al*., 2008), giving $u_{thresh} \approx 4 - 8$ ms^{-1} Eqn (1). Similar seeds have been observed to abscise when $\overline{u} > 2$ ms^{-1} (Skarpaas et al., 2006; Soons & Bullock, 2008; Greene & Quesada, 2011). If turbulence generates near-Gaussian fluctuations in u, with σ_u ranging between 1 and 2 ms^{-1}, then for $\overline{u} > 2$ ms^{-1} abscission would occur $> 5\%$ of the time. The simple rupture model is thus broadly consistent with observations (Skarpaas *et al*., 2006; Soons & Bullock, 2008; Greene & Quesada, 2011).

Assuming a Gaussian u distribution, the abscission probabilities can be derived as a function of the u^*. First, $\overline{u}$ and σ_u are expressed in terms of u^* as $\overline{u} = a_1 u^*$ and $\sigma_u = a_2 u^*$, where a_1 and a_2 are specific to the canopy geometry (see Supporting Material). Noting that $\int_{x_o}^{\infty} (1/2) \exp(-x^2) dx = (\sqrt{\pi/2}) \mathrm{erf}(x_o/\sqrt{(2)})$, Eqn (2) can be re-expressed to give the probability of abscission as a function of the hourly u^*:

$$g(u^*) = 1 - \frac{1}{2}\left[1 + \mathrm{erf}\left(\frac{u_{thresh} - a_1 u^*}{a_2 u^* \sqrt{2}}\right)\right]. \tag{3}$$

When plotted (Panel e, Fig. 1), Eqn (3) describes a dispersed form of the usual sigmoidal Gaussian cumulative density

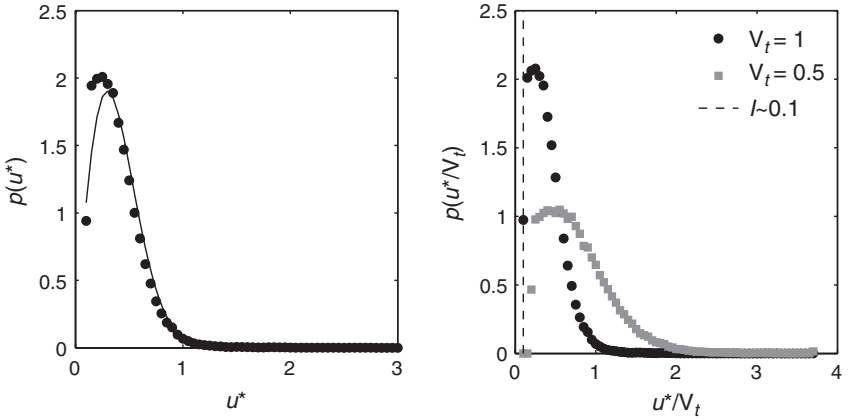

Fig. 2. Comparison of the measured u^* distribution at Duke Forest and the Weibull distribution that best fits it, on left. Eddy covariance results become unreliable at low u^*, so we fit the $u^* > 0.1$ data only. As shown in the right-hand panel, the condition $u^*/V_t > I$ is upheld in most cases, meaning that initial conditions do not influence seed trajectories.

function (CDF). The distribution of u^* values experienced by a nonrandomly abscising seed population, $p(u^*)$, is obtained by taking the product of the Weibull distribution of u^* and the abscission probability for each u^*, and normalizing the result. That is:

$$p(u^*) = \frac{Weib(u^*)g(u^*)}{\int_0^\infty Weib(u^*)g(u^*)du^*}. \quad (4)$$

The normalization in Eqn (4) assumes that all seeds disperse and all variability in u^* is sampled. In the derivation above, we assumed that the fluctuations in u' followed a true Gaussian distribution, even though the u distribution can be positively skewed (Katul *et al*., 1997) in forest canopies. Such skewness, however, does not change the sigmoidal form of $f(u)$ and $g(u^*)$, as shown in the Supporting Material.

Threshold angle and wear and tear models. Seed release conditions in the threshold angle and 'wear and tear' models are based on the motion and history of motion of seeds in the canopy. Tree movement can be approximated with an elastic beam model (Flesch & Grant, 1991) in which fluctuating wind drag initiates tree movement, which is modified by gravity, damping, and the elasticity of the wood. In this simplified model, a deflection in the tree position (quantified by the tree angle θ from the vertical) starts a swaying motion. The tree sway behavior depends on only three factors: (i) a damping coefficient ζ, (ii) a drag term F that modifies the effects of the wind speed, and (iii) the fluctuations and magnitude of the wind speed itself. Example output from the tree sway model is shown schematically in Panel b of Fig. 1, and the full model derivation is provided in the Supporting Material. The model was run for different values of the ζ, F, and a representative threshold angle for seed release θ_{thresh}, shown in Table 1. Seed abscission frequencies were computed from the rate at which $\theta > \theta_{thresh}$, and the rate at which the accumulated angular kinetic energy $(d\theta/dt)^2$ exceeded the thresholds given in Table 1. The probability of seed release from all three mechanisms was described by a generalized sigmoidal function:

$$g(u^*) = \frac{a{u^*}^b}{c + {u^*}^b}. \quad (5)$$

When $(u^*)^b >> c$, $g(u^*) \to a$. Provided that a is large enough for abscission to occur during a dispersal season, the normalization in Eqn (4) means that seed dispersal outcomes are independent of a. Eqn (5) provides a generalization of the effects of nonrandom abscission.

Inertial Particle Coupled Eulerian-Lagrangian Closure Model (IP-CELC)

IP-CELC for stationary u^*. The (CELC) model is a stochastic Lagrangian model that tracks the movement of individual fluid parcels and seeds (particles) within a neutrally stratified, turbulent flow field (Nathan & Katul, 2005; Poggi *et al*., 2006). CELC models the profiles of the first and second moments of the flow field in a Eulerian frame of reference using conventional second-order closure assumptions to explicitly account for turbulence and the presence of a vegetated canopy (Massman & Weil, 1999). Once the Eulerian flow field is computed, Lagrangian fluid and seed velocities are constructed with a set of Langevin equations whose drift and dispersion formulation preserve the Eulerian flow statistics. The model is run for an ensemble of seeds to generate probability distributions of flights. One shortcoming of the original CELC model is that it neglects the inertia of seeds, which causes seeds to 'slip' in the wind, and for the wind and seed velocities to be imperfectly coupled to each other. The CELC model was modified to account for inertial particles (Wilson, 2000; Li & Taylor, 2005). In the modified framework, the autocorrelation timescale is adjusted according to a dimensionless parameter β' that accounts for inertia as follows:

$$\Gamma_P = \frac{\Gamma}{\sqrt{1 + (\frac{\beta' V_t}{\sigma_w})^2}}, \quad (6)$$

where $\Gamma[t]$ is the Lagrangian correlation timescale of the turbulence, V_t [ms^{-1}] the terminal velocity of the seed, and σ_w[ms^{-1}] the standard deviation of the vertical velocity fluctuations. For noninertial particles that are fully coupled to the flow, $\beta' = 0$ and seeds move perfectly with the fluid. For spherical particles that slip in the flow field, $\beta' = 1.5$. The autocorrelation is applied when updating the local air velocity around the seeds, as detailed in the Supporting Material. The seed velocity dynamics in the IP-CELC model are summarized below. A full description of the fluid equations is given in the Supporting Information. The seed is accelerated or decelerated in the longitudinal (x), lateral (y), and vertical (z) directions by drag forces that arise from the difference between the velocity of the seed $\vec{v_p}(u_p, v_p, w_p)$ and the fluid, $\vec{v}(u, v, w)$, where by convention u [ms^{-1}] denotes the wind speed in the x direction, v [ms^{-1}] the speed in the y direction and w [ms^{-1}] the speed in the z direction:

$$\begin{aligned} \frac{du_p}{dt} &= A|\vec{v} - \vec{v_p}|(u - u_p) \\ \frac{dv_p}{dt} &= A|\vec{v} - \vec{v_p}|(v - v_p) \\ \frac{dw_p}{dt} &= A|\vec{v} - \vec{v_p}|(w - w_p), \end{aligned} \quad (7)$$

where $g' = g(\rho_p - \rho)/\rho_p$[ms^{-2}] is the reduced gravity experienced by the particle (with density ρ_p[kgm^{-3}]) in the fluid (with density ρ)*and* g[ms^{-2}] is the gravitational acceleration. The coefficient A[m^{-1}] is computed from the fluid drag as follows:

$$A = \frac{3}{8}\frac{\rho}{\rho_p}\frac{C_D}{r}, \quad (8)$$

Table 1. Model parameters used

Abscission	$(d\theta/dt)^2$	θ_{thresh}	Damping coefficient, ζ	F
	1, 10, 1000	$\pi/2$	0.01, 0.1, 1	0.5
IP-CELC	r	V_t	ρ_{air}	β'
	3 mm	0.5, 1, m/s	1.38 kg/m^3	0, 1.5

where $r[m]$ is the effective seed radius, and the dimensionless C_D is computed as $C_D = \frac{\alpha_1}{Re_p}(1 + \alpha_2 Re_p)$. The dimensionless particle Reynolds number, $Re_p = |\vec{v} - \vec{v_p}|d/v$, quantifies the velocity difference between the fluid and the seed. As the seed velocity approaches the air velocity $Re_p \to 0$, $C_D \to \infty$, attaching the seed to the surrounding air, and generating the noninertial case. In the limit of large particle Reynolds numbers (large slippage), the drag coefficient approaches a constant that depends on the seed morphology. Coefficients α_1 and α_2 are not known for most seeds, so typical values for smooth spheres: $\alpha_2 = 0.016$ and $\alpha_1 = 24$ were adopted. Stoke's flow was assumed to relate the seed terminal velocity to its density:

$$\rho_p = \frac{3}{8}\frac{C_{DS}}{gr}V_t^2, \tag{9}$$

where, from analysis of, for example, the data of Sudo *et al.* (2008), the Stokes drag coefficient C_{DS} is close to 0.4 (very similar to the drag coefficient of a sphere at large Re_p). Parameters used in the IP-CELC calculations are shown in Table 1.

Eulerian wind statistics: contemporary and global stilling scenarios

Contemporary conditions. The IP-CELC model requires specification of the second-order flow statistics throughout and above a vegetated canopy. This profile was simulated for a mixed hardwood canopy using an analytical second-order closure model (Massman & Weil, 1999) (see Supplementary Material). Neutral atmospheric stability and planar-homogeneous flow conditions were assumed. Representative temporal variations in u^* were taken from 10 years (1998–2008) of measurements made at the Duke Forest, located near Durham, North Carolina, USA. The Weibull distribution describing the u^* variations at Duke Forest has a scale parameter of 0.44, a shape parameter of 1.91, and a seasonal mean u^* of 0.38 ms^{-1}, equivalent to a seasonally averaged $\overline{u}$ of 1.3 ms^{-1} at the canopy top (Fig. 2).

Wind statistics with a global stilling scenario. Studies of global stilling report changes in the mean wind velocity which must be translated into changes in the (Weibull) pdf of the mean hourly wind speed. Here, it was assumed that changes in the mean wind speed due to stilling can be absorbed by the scale parameter of the distribution, leaving the shape of the distribution unaltered. The global mean annual change in surface wind speed reported by McVicar *et al.* (2012b), -0.014 $ms^{-1}a^{-1}$ was applied over time horizons of 20 and 50 years to the Weibull pdf measured at Duke forest. To accommodate these changes in the mean wind speed, the Weibull scale parameter changed from 0.44 to 0.12 (20 years) and to 0.06 (50 years).

Model implementation

To generate dispersal kernels, seed release was simulated just beneath the canopy height. Seed trajectories were computed until they arrived within 0.1 m of the $z = 0$ boundary, at which point they were assumed to have settled, and their x location was recorded. Models were run for five different seed terminal velocities ($V_t = 0.5, 0.625, 0.75, 0.875, 1.0$ ms^{-1}), two different assumptions about inertia ($\beta' = 0$ and 1.5), three canopy heights (h = 5,10 and 20 m), three different initial conditions, and 10 values of u^* spanning the Duke Forest Weibull distribution. At least 10 000 simulated seeds were released for each factorial combination of the parameters.

Nonstationary u^* in seasonal dispersal kernels. The Duke Forest u^* distribution provided the starting point for computing the effects of nonstationarity in u^* under all scenarios. The empirical u^* distribution was discretized into 10 bins. IP-CELC was run with u^* fixed at the centroid of each bin, generating 10 hourly dispersal kernels. The resulting seasonal dispersal kernel from unbiased seed release was computed as the superposition of each hourly kernel, weighted according to Weib (u^*). Nonrandom abscission was accounted for by weighting the hourly kernels with Eqn (4) rather than Weib (u^*). Seasonal kernels were generated for three kinds of abscission: (i) random abscission ($b = 0$, $c = 0$); (ii) moderately biased abscission ($b = 5$, $c = 1$); and (iii) Strongly biased abscission ($b = 15$, $c = 100$), and for three mean wind speed cases, (a) the contemporary wind environment, and the (b) 20 and (c) 50 year stilling cases. Events with probabilities $<1 \times 10^{-4}$ were assumed not to occur within a dispersal season and were set to zero.

Initial conditions on u and u_p. The effect of the initial horizontal velocities was tested with three different model runs. Unbiased initial conditions were generated by selecting u_o from a Gaussian pdf. Nonrandom initial conditions were implemented by rejecting the u_o value with probability $1-p(u)$, where $p(u)$ was generated for the simple rupture case, using four different values of $u_{thresh} : 2, 3, 7.5,$ and 15 ms^{-1}, spanning the range of possible wind speeds above a 10 m canopy. Resulting distributions of u_o were positively skewed, paralleling observations in grasses (Pazos *et al.* 2013). The initial particle velocity, u_{po} was set to either equal u_o, or to zero, bounding the physical range of possibilities. Dispersal kernels were generated for the three initial conditions: (i) unbiased u_o, $u_{po} = 0$; (ii) biased u_o, $u_{po} = 0$ and (iii) biased u_o, $u_{po} = u$.

Analysis of dispersal kernels and computation of migration rates. The seasonal dispersal kernels were characterized by their first through fourth-order moments, allowing a direct evaluation of abscission effects on seed flights. To compute the migration rates, seasonal dispersal kernels were fit with the analytical WALD model (Katul *et al.* 2005) using maximum likelihood estimators. The WALD parameters (μ, λ, see Supporting Information) are directly related to the maximum population migration rate (Thompson & Katul, 2008), and can be decomposed into contributions from the wind statistics (an effective mean wind speed u_{eff} , fluctuating vertical velocity $\sigma_{w,\text{eff}}$, and scaling constant $\kappa \approx 0.6$), and contributions from the seed characteristics:

$$\mu = \frac{u_{\text{eff}} z_r}{V_t}, \lambda = \frac{u_{\text{eff}} z_r}{2\kappa h \sigma_{w,\text{eff}}}, \tag{10}$$

where z_r is the seed release height [m], h the canopy height [m], and V_t the terminal velocity [ms^{-1}]. We used the effective

wind statistics to estimate the sensitivity of migration rates to nonrandom abscission and stilling for 15 wind-dispersed species described in Thompson & Katul (2008), Nathan *et al.* (2011a) (parameters given in Table 2). For each species, we used the IP-CELC generated with h and V_t parameters that most closely matched the properties of that species to estimate the WALD parameters and the migration rates.

Results

Abscission probabilities

Similar sigmoidal forms of the functions $f(u)$ and $g(u^*)$ could be described using Eqn (5) regardless of the specific details of the three seed release models. Typical results are shown in Fig. 3. The function $f(u)$ was steep, with an asymptote near unity for the simple rupture and deflection mechanisms, reflecting the threshold responses. The asymptote occurred at $f(u)<<1$ for the accumulated energy mechanism. This was due to the deflection angles and angular velocities being bounded. These bounds imposed a minimum timescale over which the seed-plant connection could weaken, and resulted in a lower frequency of abscission. Eqn (5) was fitted to experimental observations: five distinct wind-dispersed species studied by Jongejans *et al.* (2007), Soons & Bullock (2008), Greene & Quesada (2011) – see Fig. 4 – and described the data well, supporting the generality of the sigmoidal relationships, although fitted values of a, b, and c varied. The functional response of seed release probabilities to bias in the abscission mechanisms therefore seems to be general, presumably because abscission probabilities always derive from integration of the pdf of u'.

Table 2. Characteristics of 15 wind-dispersed tree species

	V_t, ms^{-1}	Release height (m)	Canopy height (m)
Acer rubrum	0.67	10	17
Acer saccharum	1.0	10	17
Acer negundo	0.92	9.5	19
Acer saccharinum	0.87	12.5	25
Betula lenta	1.6	15	20
Betula papyrifera	0.55	16	21
Carpinus caroliniana	0.98	8.3	11
Fraxinus americana	1.4	13	19
Fraxinus pennsylvanica	1.6	12	17
Liquidamber styraciftua	1.05	16	26
Liriodendron tulipifera	1.48	17	26
Picea glauca	0.62	17	23
Pinus strobus	0.93	34.5	46
Pinus taeda	0.7	22	31
Tilia americana	2.92	12	16

How do changes in initial conditions influence the dispersal kernels?

The moments of hourly dispersal kernels generated using the same u_0, but with $u_{p0} = 0$ in one case and $u_{p0} = u_0$ in the other, differed by only 3%. Biases in the initial velocity of the seeds due to nonrandom abscission therefore have a negligible effect on seed transport. The initial wind velocity u_0 altered the hourly dispersal kernels of heavy seeds, but only when u_{thresh} and u^* were both low. For instance, for heavy seeds, with $u_{thresh} = 2$ ms^{-1} and $u^* = 0.3$ ($\overline{u} = 1.1$ ms^{-1}), the mean travel distance was 2.5 times greater for seeds released only when $u > u_{thresh}$ than for seeds released randomly into the same wind conditions. This effect was diminished, however, for higher u^*, u_{thresh}, and for light seeds. The decline in the influence of the initial wind speed arises from two causes. First, as u^* increases with fixed u_{thresh}, the proportion of the instantaneous wind distribution truncated by the release mechanism declines. Second, to control for this effect, the ratio of the moments of the kernels was plotted as a function of the percentage truncation of the u^* pdf. Sensitivity to the initial conditions continued to decline with increasing u^*, u_{thresh}, and decreasing terminal velocity, even as the truncation of u^* became less pronounced, as shown in Fig. 5. For light seeds, initial conditions never altered the dispersal distances by more than 10%. Paradoxically, therefore, the greater the bias in initial conditions due to nonrandom abscission, the less effect it had on the subsequent seed dispersal.

How does the distribution of u^* affect dispersal kernels?

On seasonal timescales, nonrandom abscission alters dispersal by changing the distribution of u^* (Eqn (4)) experienced by dispersing seeds, due to the weighting of the u^* distribution by $g(u^*)$, the seed release probabilities (Eqn (5)). Figure 6 shows the effect of varying b and c on $g(u^*)$, and on the mean seasonal dispersal length for light, inertial particles. The trends are representative of all values of V_t and β'. Low b values and low c values recover random abscission (near-uniform probability of seed release for all u^*). All other cases lead to an increase in abscission frequency with u^*, increasing the mean dispersal distance μ. The effect of $g(u^*)$ on the higher order moments of the light, inertial particle dispersal kernels is shown in Fig. 7. Like the mean, the variance of the dispersal kernel increased as abscission became more biased. This trend was reversed, however, for the third- and fourth-order moments. Although the kernel was always positively skewed and leptokurtic, both the skewness and kurtosis declined as abscission was biased toward high u^*.

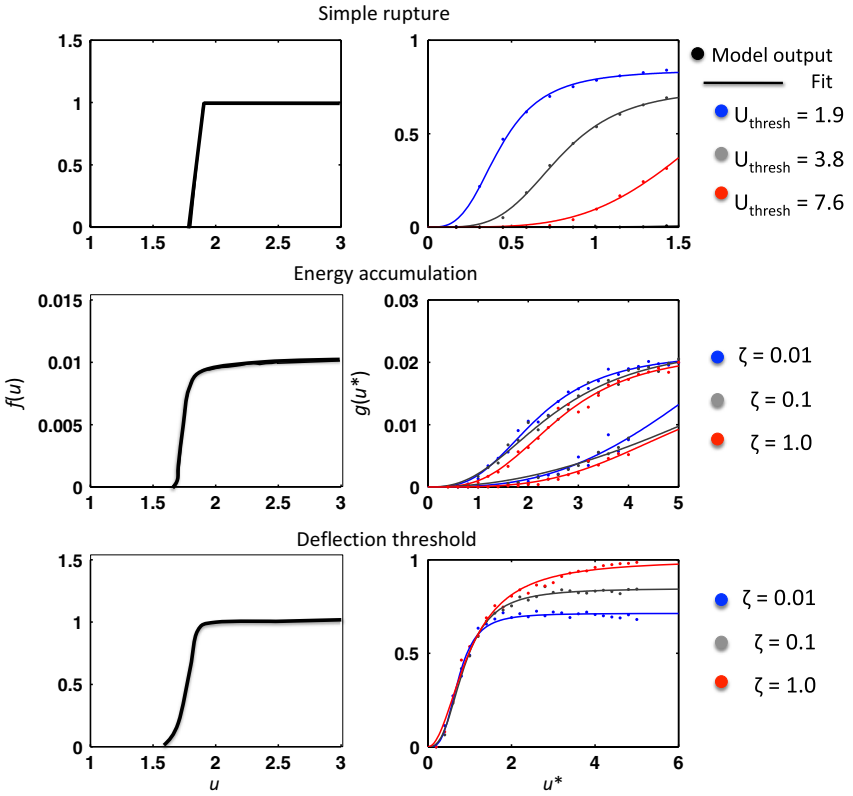

Fig. 3. Results from the abscission models. The left-hand column shows the probability of seed release as a function of the instantaneous horizontal wind speed, u, which describes a step-function in all cases. For the simple rupture and threshold angle models, release probabilities approached 100% at high u. For the energy accumulation model, the saturating probability was $< 100\%$. The right-hand column shows the frequency of release events with varying u^*, a sigmoidal function in all cases.

The decrease was particularly dramatic (around two orders of magnitude) in the kurtosis.

Effect of different seed and canopy properties on the predicted seed dispersal kernels

Seed properties altered the absolute value of the moments of the dispersal kernels, although the trends in these moments with $g(u^*)$ were consistent. Increased terminal velocity (predictably) resulted in shorter dispersal distances regardless of β'. The lower order moments of the kernels were sensitive to the seed terminal velocity as shown in Table 3: the mean, for example, scaled with $1/V_t$, in agreement with the predictions of the WALD model (Katul *et al.*, 2005). This scaling was preserved across the range of nonrandom abscission behaviors treated, suggesting that even the composite monthly dispersal kernels generated by the convolution of the Weibull (or truncated Weibull) and the hourly dispersal kernels preserved the general behavior of a Wald Distribution. For all terminal velocities with $h = 10$, changing β' altered the moments of the kernels by 5%–10%. The limited sensitivity of the kernels to the specification of inertial or noninertial behavior by the seeds indicates that the timescales over which the wind was able to accelerate seeds were short compared to the timescale on which seeds would reach the ground. Consistent with this interpretation, the moments of inertial and noninertial kernels differed on average by 19% for $h = 5$, by 12% for $h = 10$ and by 6% for $h = 20$, suggesting that as the timescale for seeds to fall increases, the effect of inertia declines. As shown in Table 3, the inertial seeds were typically more sensitive to the effects of nonrandom abscission than were the noninertial seeds, suggesting that the longer response timescales of these seeds tends to exaggerate long-distance dispersal. Higher canopies exaggerated long-distance dispersal effects, with the kurtosis of the kernels scaling near-linearly with the inverse of the canopy height – again as would be anticipated if the dispersal behavior approximated a Wald Distribution. The damping of these effects arises in part because the wind statistics as well as the seed environment scale with the canopy height. The overall sensitivity of the kernels to the properties of seeds and canopies was consistent with the predictions based on Wald Distribution (Katul *et al.*,

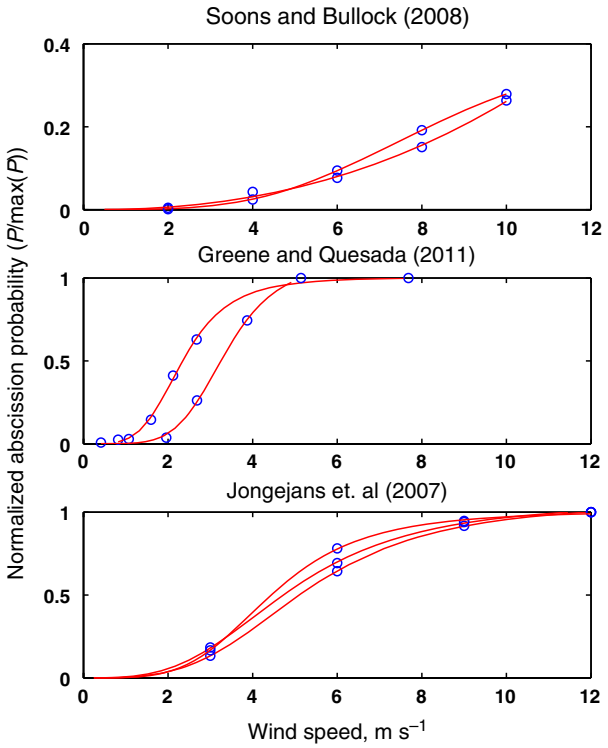

Fig. 4. Experimentally estimated abscission probabilities vary with the mean wind speed according to the proposed sigmoidal $g(u^*)$ function. Data presented include the mean of measurements from Soons & Bullock (2008); updraft and longitudinal wind speed tests from Greene & Quesada (2011) and measurements made for peak turbulence and temperature test cases by Jongejans *et al.* (2007). Abscission probabilities were normalized by their maxima, allowing different curves to be plotted on the same axes.

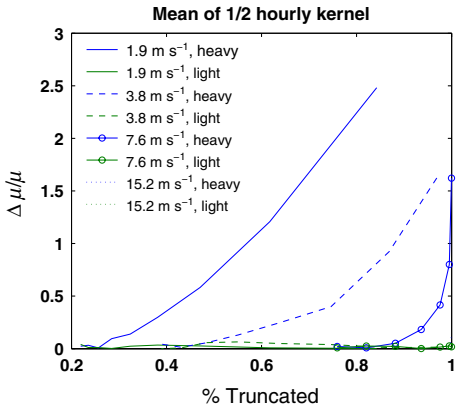

Fig. 5. Change in the mean dispersal distance for nonrandom abscission relative to the mean dispersal distance for random abscission; inertial particles. The change in dispersal distance is plotted as a function of the % of the ambient wind speed PDF that is truncated by applying a threshold for seed release. As the release thresholds increase, the overall wind speed profile also increases, reducing the influence of the initial conditions on the dispersal trajectories.

2005), even when there was considerable variation in the hourly mean wind speed. This provides justification in proceeding to use the WALD model to estimate migration behavior.

WALD kernels and migration rates

Figure 8 shows the sensitivity of the migration rates for the wind-dispersed species in Table 2 grouped according to the wind conditions (current, 20 years stilling, 50 years stilling): quantitative details are presented in Table 4. The changes in potential migration rate were strongly influenced by canopy height and seed terminal velocity: the higher the terminal velocity the less sensitive the migration rate was to changing ambient wind conditions and nonrandom abscission. For heavy seeds, however, high canopies lead to a greater sensitivity of the migration rates to nonrandom abscission and stilling. For light seeds, nonrandom abscission affected migration rates most greatly for trees with high canopies. These changes were largely independent of β'. Reductions in mean wind speed reduced potential migration rates, most strongly for the 50-year stilling case. Migration rates of several species were dramatically sensitive to nonrandom abscission: strongly biased abscission increased the maximum potential migration rates by factors of 100–200. These increases were strongly sensitive to the wind conditions: stilling scenarios over a 50-year time-frame effectively eliminated the effects of nonrandom abscission on migration. Nonrandom abscission therefore appears to have the potential to cause strongly nonlinear dependence of dispersal behavior and population migration potential on mean wind speed conditions.

The ecological implications of this nonlinear sensitivity can be explored through a synthetic example using some well-characterized wind-dispersed species. The synthetic nature of the example arises from the limited data regarding nonrandom abscission in realistic plant communities. The example consists of the migration potential of an assemblage consisting of silver maple *Acer saccharinum*, white ash *Fraxinus americana*, and loblolly pine *Pinus taeda*, three distinct wind-dispersed tree species that currently grow in the Eastern USA. Greene & Johnson (1992) estimated that the abscission probability of silver maple seeds was related to the wind speed as $f(u) = 0.0022u^{2.31}$ (with u in [ms^{-1}]). Delcourt & Delcourt (1987) provide estimated population migration velocities for these species from the palynological record: approximately, 163 m yr^{-1} for silver maple, 123 m yr^{-1} for white ash and 240 m yr^{-1} for loblolly pine. These velocities are consistent with those

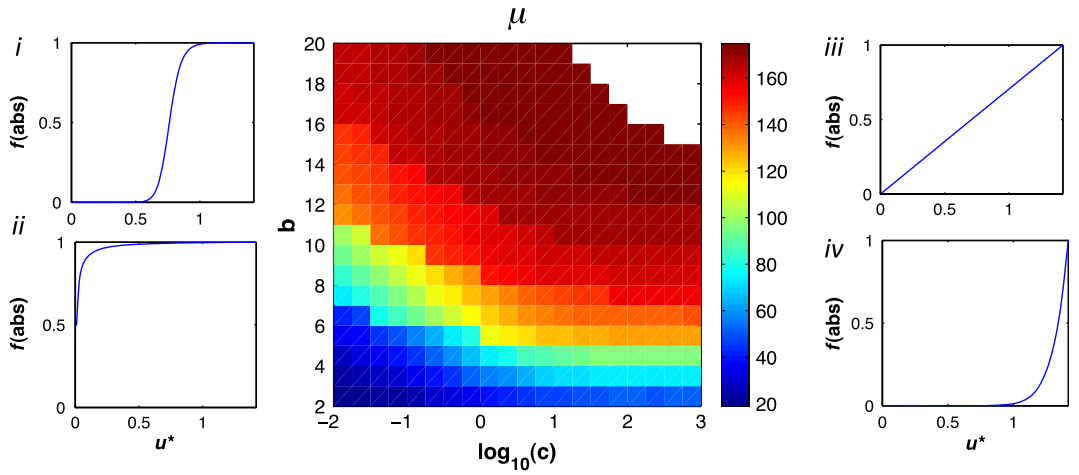

Fig. 6. Effect of varying the parameters b and c on the frequency of abscission as a function of u^* (panels i–iv) and on the overall mean dispersal length μ for light, inertial particles (main panel). The $g(u^*)$ functions in panels i–iv are normalized by their maximum values. High b and low c values (panel i) yield a sigmoid. Low b and low c lead to near-uniform abscission probabilities, recovering the random seed release case. High c and high b values (iii) lead to a near-linear increase in abscission frequency but with absolute value <0.0001, interpreted as no abscission (white region in the center panel). Finally, high c but low b values (panel iv) result in a power-law increase in the abscission probability with u^*, which does not saturate for physically reasonable u^* values.

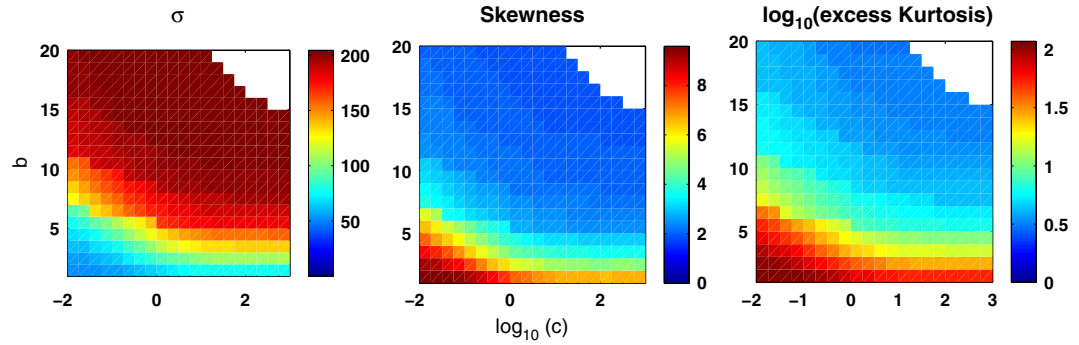

Fig. 7. Moments of the dispersal kernel for inertial particles with $V_t = 0.5$ ms^{-1}. The mean, standard deviation, skewness, and base 10 logarithm of the excess kurtosis are shown.

predicted from the WALD model using the seed and growth properties of these species and the wind statistics of the contemporary eastern USA computed from Ameriflux towers (Thompson & Katul, 2008). The historical migration velocities are therefore taken as reasonable estimate of the current migration potential of these three species. We computed the dispersal kernels and migration velocities for the three species after 20 and 50 years of stilling, assuming firstly random abscission, and second that all the plants exhibit the same abscission behavior as the silver maple. Results are illustrated in Fig. 9.

Under contemporary conditions, loblolly pine migrates nearly twice as fast as the other two trees. If it established successfully, then the two slower hardwood species would migrate into an establishing coniferous forest. This pattern is similar to the normal successional sequence in south-eastern forests (Stoy *et al.*, 2006), suggesting that all species would ultimately spread in this scenario. If, however, the invasion did not commence for 20 years, during which time the stilling trend continued, then the loblolly pine and white ash would migrate at similar rates (assuming random seed abscission). Seedling competition between the two species could then determine the nature of the forest that the slowly migrating maple would invade, and the likely success of that invasion. Finally, under a scenario where all trees abscise nonrandomly and the stilling trend continues for 50 years, the maple and ash populations would outpace the pine. Successful migration of all three species would depend on whether a pioneer species (loblolly pine) could successfully invade a later-successional forest assemblage (hardwoods). Typical successional dynamics suggest that this process would

Table 3. Range in the mean, standard deviation, skewness, and excess kurtosis for seeds released from 10 m canopies at five different terminal velocities, over the range of b and c parameters that defined the synthetic $f(u)$ functions

	μ		σ		Skewness		Excess kurtosis	
	Min	Max	Min	Max	Min	Max	Min	Max
$\mathbf{V}_t = 1, \boldsymbol{\beta}' = 1.5$	7.12	138	23.2	274	3.77	33.6	19.5	1950
$\mathbf{V}_t = 0.875, \boldsymbol{\beta}' = 1.5$	8.45	201	34.1	406	3.77	34.1	19.7	2010
$\mathbf{V}_t = 0.75, \boldsymbol{\beta}' = 1.5$	10.6	305	52.3	622	3.49	32.3	15.8	1730
$\mathbf{V}_t = 0.625, \boldsymbol{\beta}' = 1.5$	14.6	460	81.3	929	3.43	29.1	15.2	1420
$\mathbf{V}_t = 0.5, \boldsymbol{\beta}' = 1.5$	22.7	805	142	1520	3.06	25.4	12.3	1060
$\mathbf{V}_t = 1, \boldsymbol{\beta}' = 0$	7.56	117	20.7	249	4.17	36.5	24.4	2380
$\mathbf{V}_t = 0.875, \boldsymbol{\beta}' = 0$	8.63	171	30.1	365	4.07	36.3	22.8	2290
$\mathbf{V}_t = 0.75, \boldsymbol{\beta}' = 0$	10.5	240	45.1	506	3.62	31.0	16.6	1550
$\mathbf{V}_t = 0.625, \boldsymbol{\beta}' = 0$	13.9	405	74.1	850	3.47	30.2	15.5	1500
$\mathbf{V}_t = 0.5, \boldsymbol{\beta}' = 0$	21.1	708	132	1430	3.31	27.3	14.6	1230

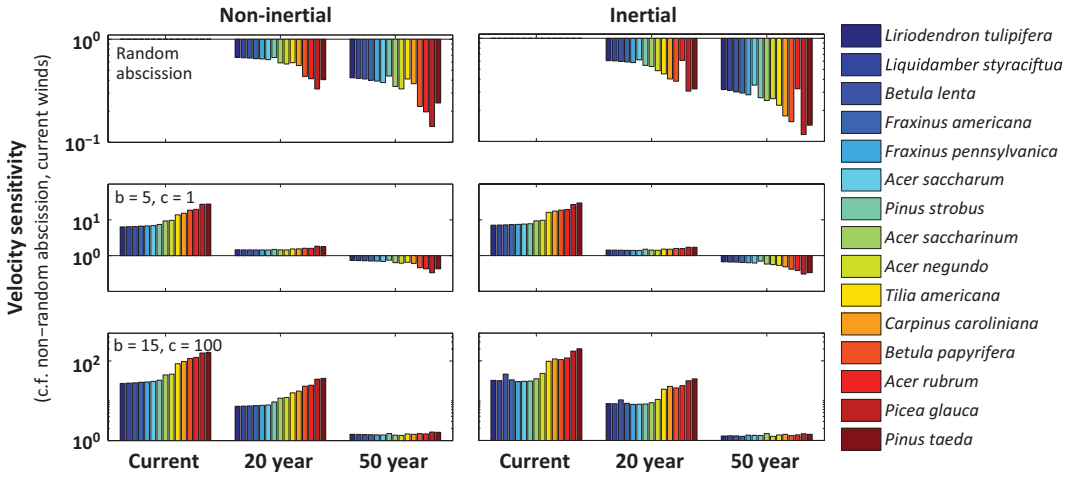

Fig. 8. Effect of nonrandom abscission (three cases shown: random, a gentle sigmoidal function with $b = 5, c = 1$, and an abrupt sigmoidal function with $b = 15, c = 100$) and stilling on the migration rates of 15 tree species, normalized to the case of random abscission with contemporary wind statistics. Kernels reflect the canopy height, seed release height and terminal velocity of the tree species. Predictions based on noninertial kernels are shown on the left, inertial kernels on the right: the trends in migration velocity with stilling are largely comparable for the two sets of assumptions.

likely be slow, dependent on disturbance, and thus not conducive to spreading of the pine population. This example, although synthetic, illustrates the potential for different combinations of stilling and nonrandom abscission applied to an assemblage of wind-dispersed species to generate different patterns of migration. Given the nonlinear competition and survival dynamics between different species at different life stages, the long-term composition of areas subject to invasion by wind-dispersed species could vary dramatically based on these invasion patterns. At a minimum, given the current understanding of *A. saccharinum*, stilling combined with the nonrandom abscission of the maple seeds could slow migration from the historical 163 m yr^{-1} to as little 16 m yr^{-1}. Predictions that ignore the current habit of nonrandom abscission would overestimate the future migration rate by a factor of three.

Discussion

The aim of this study was to (i) provide a theoretical basis for empirical relationships between abscission and the wind environment (Greene & Johnson, 1992; Greene, 2005; Skarpaas *et al*., 2006; Jongejans *et al*., 2007; Soons & Bullock, 2008; Bohrer *et al*., 2008; Greene & Quesada, 2011); (ii) to determine the dominant factors that influence the form of dispersal kernels formed when seeds abscise nonrandomly (Greene, 2005); and (iii) to investigate the joint effects of nonrandom abscission and a slowing near-surface wind environment on dispersal and population migration rates (McVicar *et al*., 2008; Loarie *et al*., 2009; Guo *et al*. 2011; McVicar *et al*., 2012b, a).

The results demonstrate that abscission probabilities depend on the integrated pdf of the instantaneous wind

Table 4. Sensitivity of migration rates of 15 wind-dispersed tree species to nonrandom abscission and stilling. Inertial (In.) and Non-Inertial (NI) data shown separately. Two nonrandom abscission cases are illustrated

	Current wind speed					25 Year simulated stilling						50 Year simulated stilling					
	Rd.	$b = 5$, $c = 1$		$b = 15$, $c = 100$		Rd.		$b = 5$, $c = 1$		$b = 15$, $c = 100$		Rd.		$b = 5$, $c = 1$		$b = 15$, $c = 100$	
		In.	NI	In.	NI	In.	NI	In.	NI	In.	NI	In.	NI	In.	NI	In.	NI
Acer rubrum	1	19	20	120	120	0.38	0.41	1.6	1.6	24	25	0.16	0.20	0.38	0.43	1.4	1.5
Acer saccharum	1	7.6	6.9	33	31	0.58	0.63	1.4	1.4	8.6	7.9	0.28	0.38	0.62	0.69	1.3	1.4
Acer negundo	1	9.6	9.7	48	47	0.53	0.57	1.4	1.4	11	12	0.25	0.33	0.56	0.62	1.3	1.3
Acer saccharinum	1	9.4	9.3	47	45	0.55	0.59	1.4	1.4	10	12	0.27	0.35	0.58	0.64	1.3	1.4
Betula lenta	1	7.2	6.5	31	28	0.60	0.66	1.4	1.4	8.2	7.4	0.31	0.41	0.65	0.72	1.3	1.4
Betula papyrifera	1	19	19	110	110	0.40	0.44	1.6	1.6	23	23	0.18	0.22	0.41	0.46	1.4	1.5
Carpinus caroliniana	1	17	15	110	97	0.45	0.56	1.5	1.6	21	18	0.22	0.37	0.48	0.61	1.3	1.4
Fraxinus americana	1	7.4	6.7	32	29	0.60	0.65	1.4	1.4	8.4	7.6	0.30	0.40	0.64	0.71	1.3	1.4
Fraxinus pennsylvanica	1	7.4	6.8	32	30	0.59	0.64	1.4	1.4	8.5	7.7	0.29	0.39	0.63	0.70	1.3	1.4
Liquidambar styraciftua	1	7.1	6.4	31	28	0.61	0.66	1.4	1.4	8.1	7.3	0.32	0.42	0.66	0.73	1.3	1.4
Liriodendron tulipifera	1	7.1	6.4	30	27	0.61	0.66	1.4	1.4	8.1	7.3	0.32	0.42	0.67	0.73	1.4	1.4
Picea glauca	1	27	27	180	159	0.31	0.33	1.7	1.8	32	35	0.12	0.14	0.30	0.33	1.5	1.6
Pinus strobus	1	7.8	7.4	36	33	0.62	0.66	1.5	1.5	8.8	9.3	0.35	0.44	0.70	0.74	1.5	1.5
Pinus taeda	1	30	28	200	160	0.32	0.41	1.7	1.8	35	37	0.14	0.24	0.33	0.43	1.4	1.6
Tilia americana	1	16	14	97	85	0.49	0.59	1.5	1.5	19	16	0.26	0.41	0.53	0.65	1.4	1.5
Mean	1	13	12	76	68	0.51	0.57	1.5	1.5	16	15	0.26	0.35	0.55	0.62	1.4	1.5
Min	1	7.1	6.4	30	27	0.31	0.33	1.4	1.4	8.1	7.3	0.12	0.14	0.30	0.33	1.3	1.3
Max	1	30	28	200	160	0.62	0.66	1.7	1.8	35	37	0.35	0.44	0.70	0.74	1.5	1.6

speed for three different mechanisms tested, and that due to the near-Gaussian form of this PDF, sigmoidal (error-function-like) relationships between abscission probability and wind speed are likely to be general regardless of the abscission mechanism. Nonrandom abscission, as expected, increased dispersal length scales and potential plant population migration rates, primarily by truncating the pdf of u^* experienced by dispersing seeds (Pazos *et al*., 2013). Although nonrandom abscission positively biased the initial conditions experienced by seeds, this bias only influenced seed trajectories under low wind speed conditions, mitigating the effect of the change in initial conditions. Similarly, although nonrandom abscission increased the mean wind speed experienced by dispersing seeds, it reduced the variability in the wind speed distribution, and thus the kurtosis of the dispersal kernel. Seeds released under nonrandom conditions therefore travel further as a population, but are less likely to take long excursions from the modal behavior of the population. As highlighted by Clark *et al.* (1998), Clark (1998), and Nathan *et al.* (2011b), truncation of these long excursions slows the rate of population migration relative to a scenario where the mean travel distance increased without a reduction in the kurtosis of the kernel. Thus, biological and physical tradeoffs limit the extent to which nonrandom abscission can accelerate population migration rates. Finally, the effects of nonrandom abscission were strongly sensitive to the statistics of the ambient wind environment. Changes that lower ambient wind speeds, such as the observed global stilling phenomenon, disproportionately inhibit the dispersal and migration of seeds with biased release when compared to seeds that are released randomly. As illustrated in the synthetic case study, these interactions can determine community composition and patterns of invasion and migration that change as a function of global stilling scenarios and the abscission characteristics of individual species.

Tradeoff 1: bias in initial condition vs. sensitivity to initial conditions

Although nonrandom abscission biases the initial wind speeds experienced by dispersing seeds, seed trajectories become decoupled from these initial conditions as u^* increases. Therefore, the more biased the initial condition due to nonrandom dispersal, the less it affects the overall dispersal kernel. Low sensitivity to initial conditions can be attributed to the relatively long-flight times of dispersing seeds and can be interpreted via a scaling argument. The seed fall time is on the order of $\tau = h/V_t$. The integral timescale of eddies inside dense canopies is on the order of $t' = Ih/u^*$, where h is the canopy height and $I \approx 0.1$ is a parameter describing the integral timescale of the flow (see Lai *et al*., 2002).

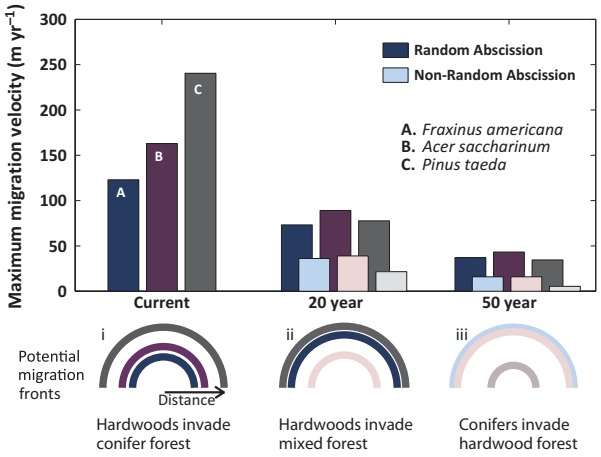

Fig. 9. Example of *Acer saccharinum* (silver maple), which Greene & Johnson (1992) showed exhibits nonrandom abscission, and which the pollen fossil record suggests exhibited an historical population migration rate of approximately 160 myr^{-1} (Delcourt & Delcourt, 1987). *Fraxinus americana* (ash) and *Pinus taeda* (loblolly pine) migration rates are shown for reference. Dark-shaded bars in the figure indicate the projected migration rates of all species under stilling scenarios assuming that they undergo random abscission. Light shaded bars indicate the same scenarios but now assuming that all species undergo nonrandom abscission with the same u dependency identified for *A. saccharinum*. Cases (i) to (iii) illustrate three different but plausible migration patterns that could result if these three species were migrating together: (i) the contemporary case in which maple and ash must invade pine forests; (ii) a 20 year scenario in which pine and ash continue to abscise randomly, but the interaction between nonrandom abscission and stilling stalls the migration of maple; and (iii) a 50 year scenario assuming all plants undergo similar nonrandom abscission. Now the pine migration is stalled, and ash and maple (slowly!) migrate together.

Whenever the seed fall timescale exceeds the eddy timescale, that is, $\tau/t' >> 1$, significant velocity fluctuations or uplift can occur, causing seed flights to 'lose memory' of the initial condition. For $\tau/t' >> 1$, we require that $u^*/V_t > 1$. Nonlinear abscission truncates small values of u^*, increasing u^*/V_t and causing the initial conditions to become decoupled from the transport behavior of most seeds, as illustrated by Fig. 5. The primary consequence of the low sensitivity to initial conditions is that the effects of nonrandom abscission on dispersal arise primarily at seasonal timescales, due to changes in the distribution of u^* during dispersal.

Tradeoff 2: increase in mean dispersal distance vs. decrease in kurtosis of dispersal kernels

At seasonal timescales, nonrandom abscission tends to truncate the lower component of the u^* pdf. By limiting abscission to high wind speeds, nonrandom dispersal increases the mean seasonal value of u^* compared to random dispersal scenarios, increasing the mean dispersal distance (Bohrer *et al.*, 2008; Maurer *et al.* 2013). Truncation of the Weibull distribution of u^*, however, makes the resulting distribution more uniform in nature. By converting the Weibull to a near-uniform distribution, nonrandom abscission removes the potential for interactions between the tails of the Weibull and Wald distributions (Thompson *et al.*, 2008), reducing the kurtosis of the seasonal kernel. This interpretation is supported by recent results of Pazos *et al.* (2013, in review), who investigated two different shapes for a u^* distribution. Nonrandom abscission truncated the low u^* probabilities. If the u^* distribution was strongly skewed toward low u^*, the truncated distribution was near-uniform. Dispersing seeds thus experienced a wide range of wind speeds, leading to a fat-tailed dispersal kernel. Conversely, where the u^* distribution was skewed toward high u^*, a small range of u^* values near the truncation threshold dominated the u^* distribution. Dispersing seeds experienced a largely uniform wind environment, and the resulting kernels were more platykurtic.

In this context, the value of nonrandom abscission as an evolutionary strategy to promote long-distance dispersal may also be limited by biological factors rather than physical processes. Requiring ever-higher wind speed conditions for seed release risks never releasing the seeds at all, exposing them to predation; or releasing seeds under conditions corresponding to extreme weather events which may be conducive to long-distance transport, but probably not to successful seed lodging and germination. Selective pressure on seeds lies in maximizing recruitment success, rather than maximizing dispersal length scales per se. Assuming that increased dispersal improves recruitment success, there are three pathways plants can adopt: (i) developing specialized dispersal structures; (ii) biasing seed release; and/or (iii) decreasing seed size to lower V_t. Of these three options, correlations between seed size and germination success are well documented, if complex (Westoby *et al.*, 1992; Jakobsson & Eriksson, 2003; Gomez, 2004; Moles & Westoby, 2004). One value of nonrandom abscission for seeds may lie in boosting dispersal length scales without requiring reductions in seed mass. Quantifying seed abscission bias between different plant species, seed masses and release heights could offer insight into the variation in the significance of seed abscission conditions between species, and thus into the significance of transport and biological tradeoffs in shaping abscission behavior.

Tradeoff 3: vulnerability to changing wind statistics

Strongly biased seed release promoted large maximum migration rates when investigated in the context of the contemporary wind environment, as shown in Fig. 8. However, it was also apparent that this release strategy was associated with sensitivity to global stilling scenarios: up to 200-fold declines in migration rates were predicted if stilling trends were to continue for 50 years. Conversely, the average reduction in migration velocity due to stilling for random seed abscission was 50%. As illustrated for the case of *Acer saccharinum*, when changing migration rates are considered across a heterogeneous community of wind-dispersed plants, the interaction between abscission and stilling can also impact the composition of migrating plant communities. Given the significance of founder effects and species-level interactions, different wind environments and species-level differences in abscission behavior could produce drastically different long-term ecological trajectories. Clearly, the importance of these effects depends on very uncertain parameters, in particular the current seed abscission and transport behavior and the persistence of the global stilling trend. There are relatively few observations that characterize species-specific abscission behavior (Greene & Johnson, 1992; Greene, 2005; Skarpaas *et al*., 2006; Bohrer *et al*., 2008; Soons & Bullock, 2008; Greene & Quesada, 2011; Maurer *et al*., 2013). The abscission behavior explored here neglected environmental conditions such as humidity and maturation schedules all of which alter abscission and may well enhance migration (Greene & Johnson, 1992; Skarpaas *et al*., 2006; Jongejans *et al*., 2007; Maurer *et al*., 2013). Field technologies for observing plant populations, tracking release dynamics, and monitoring dispersing seeds are rapidly improving (Hamilton *et al*., 2007), and there is great scope to improve understanding of abscission by detailed observational studies across multiple species. The implications for seed migration can be assessed with increasing fidelity by drawing on statistics of the friction velocity over many different canopy types representing different climatic zones and ecosystems, which are now widely available due to the increasing deployment of eddy covariance technologies (Baldocchi *et al*., 2001), or which can be estimated from canopy leaf profiles generated by high resolution and multiwaveform LIDAR is available to profile the distribution of leaf density within canopies (Lefsky *et al*. 2002; Wei *et al*., 2012). Even the second-order controls on migration imparted by the seed drag and inertial properties can be inferred by confronting high resolution particle tracking models like CELC with wind tunnel transport data.

Future work should also address the ongoing changes in the near-surface wind environment, including analysis of how the observed trends in global average wind speeds are translated into changes in the hourly wind speeds pdfs, which is currently unclear. Vautard *et al*. (2010) found that the changes in average wind speed were reflected by declines in extreme wind speeds in some regions, but not universally. Klink (1999) found that the decline in mean wind speeds was accompanied by an increase in monthly maxima in 160 stations in the USA. The validity, causes and future trajectories of wind speed stilling merit further research in their own right (McVicar *et al*., 2012b), and clarifying these issues will sharpen the implications for seed dispersal. For example, if observed trends in global wind speeds arise from increased vegetation cover, then the effects on the forest canopy species addressed in the case study may be less than indicated by the global data, since existing forests are unlikely to further increase in aerodynamic roughness. If stilling is attributed to other causes, then it has the potential to alter predictions of plant migration and adaptation to future climate scenarios. The significance of these changes will likely increase if the stilling trend continues. However, even if the observed trends in near-surface wind speed are not maintained in future decades, the results here assist in understanding wind-mediated plant migration during the period of stilling over the past 50 years.

Conclusion

This study demonstrated that multiple abscission mechanisms lead to a single functional relationship between abscission frequency and friction velocity, resulting in a monotonic increase in mean dispersal distance and population migration rate, but decrease in the kurtosis of dispersal kernels when seed releases are biased. These changes can be attributed to the moving seeds sampling a small and biased fraction of the overall hourly wind speed variability, with limited effects of the initial wind velocity and initial seed velocity on the resulting dispersal kernels. Despite the complexity of the resulting dispersal kernels, the analytical WALD model remained a valuable tool to investigate scaling of the dispersal kernels with seed and canopy properties. For a suite of tested species, nonrandom abscission increased potential migration by 1–2 orders of magnitude. This increase was not robust in the face of nonstationary wind conditions. When confronted with global stilling, all wind-dispersed plant migration rates are likely to decrease, but the decreases for randomly abscising species were on the order of 50% vs. a 200-fold reduction for the most extreme nonrandom abscission

scenarios. Species-level features relating to seed velocity and canopy structure mean that different (synthetic) combinations of abscission and stilling dynamics lead to different predictions about founding plant communities, subsequent patterns of succession and invasion, and the timescales on which these changes can occur. Characterizing abscission dynamics for key wind-dispersed species provides an opportunity to refine existing predictions about migration and climate change (e.g., Nathan *et al*., 2011a) based on the highly nonlinear interactions of stilling and abscission bias.

Acknowledgements

Support from the National Science Foundation (NSF EAR-1013339 and NSF-AGS-110227), the United States Department of Agriculture (2011-67003-30222), the United States Department of Energy (DOE) through the Office of Biological and Environmental Research (BER) – the Terrestrial Ecosystem Science (TES) program (DE-SC0006967), and the Binational Agricultural Research and Development (BARD) Fund (Award No. IS-4374-11C) are acknowledged.

References

Baldocchi D, Falge E, Gu L, et al. (2001) Fluxnet: a new tool to study the temporal and spatial variability of ecosystem-scale carbon dioxide, water vapor, and energy flux densities. *Bulletin of the American Meteorological Society*, **82**, 2415–2434. doi: 10.1175/1520-0477.

Batchelor GK (1967) *An Introduction to Fluid Dynamics*, vol. 1. 3rd edn. Cambridge University Press, New York.

Bohrer G, Katul GG, Nathan R, Walko RL, Avissar R (2008) Effects of canopy heterogeneity, seed abscission and inertia on wind-driven dispersal kernels of tree seeds. *Journal of Ecology*, **96**, 569–580. doi: 10.1111/j.1365-2745.2008.01368.x.

Chu CR, Parlange MB, Katul GG, Albertson J (1996) Probability density functions of turbulent velocity and temperature in the atmospheric surface layer. *Water Resources Research*, **32**, 1681–1688. doi: 10.1029/96WR00287.

Clark JS (1998) Why trees migrate so fast: confronting theory with dispersal biology and the paleorecord. *American Naturalist*, **152**, 204–224. doi: 10.1086/286162.

Clark JS, Fastie C, Hurtt G, et al. (1998) Reid's paradox of rapid plant migration – dispersal theory and interpretation of paleoecological records. *Bioscience*, **48**, 13–24. doi: 10.2307/1313224.

Clark JS, Lewis M, Horvath L (2001) Invasion by extremes: population spread with variation in dispersal and reproduction. *American Naturalist*, **157**, 537–554. doi: 10.1086/319934.

de Langre E (2008) Effects of wind on plants. *Annual Review of Fluid Mechanics*, **40**, 141–168. doi: 10.1146/annurev.fluid.40.111406.102135.

Delcourt PA, Delcourt HR (1987) Late-Quaternary dynamics of temperate forests: applications of paleoecology to issues of global environmental change. *Quaternary Science Reviews*, **6**, 129–146. doi: 10.1016/0277-3791.

Finnigan JJ (2000) Turbulence in plant canopies. *Annual Review of Fluid Mechanics*, **32**, 519–571. doi: 10.1146/annurev.fluid.32.1.519.

Flesch T, Grant R (1991) The translation of turbulent wind energy to individual corn plant motion during senescence. *Boundary Layer Meteorology*, **55**, 161–177. doi: 10.1007/BF00119332.

Gomez JM (2004) Bigger is not always better: conflicting selective pressures on seed size in Quercus ilex. *Evolution*, **58**, 71–80. doi: 10.1111/j.0014-3820.2004.tb01574.x.

Greene DF (2005) The role of abscission in long-distance seed dispersal by the wind. *Ecology*, **86**, 3105–3110.

Greene DF, Johnson EA (1992) Fruit abscission in Acer saccharinum with reference to seed dispersal. *Canadian Journal of Botany-Revue Canadienne De Botanique*, **70**, 2277–2283. doi: 10.1139/b92-283.

Greene DF, Quesada M (2011) The differential effect of updrafts, downdrafts and horizontal winds on the seed abscission of Tragopogon dubius. *Functional Ecology*, **25**, 468–472. doi: 10.1111/j.1365-2435.2010.01788.x.

Guo H, Xu M, Hu Q (2011) Changes in near-surface wind speed in China:1969–2005. *International Journal of Climatology*, **31**, 349–358. doi: 10.1002/joc.2091.

Hamilton MP, Rundel PW, Allen MA, Kaiser W, Estrin D, Graham E (2007) New approaches in embedded networked sensing for terrestrial ecological observatories. *Environmental Engineering Science*, **24**, 192–204. doi: 10.1089/ees.2006.0045.

Hedderson N, Balsamo RA, Cooper K, Farrant JM (2009) Leaf tensile properties of resurrection plants differ among species in their response to drying. *South African Journal of Botany*, **75**, 8–16. doi: 10.1016/j.sajb.2008.06.001.

Higgins SI, Richardson DM (1999) Predicting plant migration rates in a changing world: the role of long-distance dispersal. *The American Naturalist*, **153**, 464–475. doi: 10.1086/303193.

Hubbell SP (1980) Seed predation and the coexistence of tree species in tropical forests. *Oikos*, **35**, 214–229.

Jakobsson A, Eriksson O (2003) A comparative study of seed number, seed size, seedling size and recruitment in grassland plants. *Oikos*, **88**, 494–502. doi: 10.1034/j.1600-0706.2000.880304.x.

Jongejans E, Pedatella NM, Shea K, Skarpaas O, Auhl R (2007) Seed release by invasive thistles: the impact of plant and environmental factors. *Proceedings of the Royal Society B-Biological Sciences*, **274**, 2457–2464. doi: 10.1098/rspb.2007.0190.

Katul GG, Hsieh CI, Kuhn G, Ellsworth D, Nie D (1997) Turbulent eddy motion at the forest-atmosphere interface. *Journal of Geophysical Research*, **102**, 13409–13421. doi: 10.1029/97JD00777.

Katul GG, Porporato A, Nathan R, et al. (2005) Mechanistic analytical models for long-distance seed dispersal by wind. *American Naturalist*, **166**, 368–381. doi: 10.1086/432589.

Klink K (1999) Trends in mean monthly maximum and minimum surface wind speeds in the co-terminous United States. *Climate Research*, **13**, 193–205.

Kuparinen A, Markkanen T, Riikonen H, Vesala T (2007) Modeling air-mediated dispersal of spores, pollen and seeds in forested areas. *Ecological Modelling*, **208**, 177–188. doi: 10.1016/j.ecolmodel.2007.05.023.

Lai CT, Katul GG, Butnor J, Ellsworth D, Oren R (2002) Modeling night-time ecosystem respiration by a constrained source optimization method. *Global Change Biology*, **8**, 124–141. doi: 10.1046/j.1354-1013.2001.00447.x.

Lefsky MA, Cohen WB, Parker GG, Harding DJ (2002) Lidar remote sensing for ecosystem studies. *Bioscience*, **52**, 19–30. doi: 10.1641/0006-3568.

Li PY, Taylor PA (2005) Three-dimensional Lagrangian simulation of suspended particles in the neutrally stratified atmospheric surface layer. *Boundary-Layer Meteorology*, **116**, 301–311. doi: 10.1007/s10546-004-2731-6.

Loarie SR, Duffy PB, Hamilton H, Asner GP, Field CB, Ackerly DD (2009) The velocity of climate change. *Nature*, **462**, 1052–1055. doi: 10.1038/nature08649.

Massman WJ, Weil JC (1999) An analytical one-dimensional second-order closure model of turbulence statistics and the Lagrangian time scale within and above plant canopies of arbitrary structure. *Boundary-Layer Meteorology*, **91**, 81–107. doi: 10.1023/A:1001810204560.

Maurer KD, Bohrer G, Medvigy D, Wright SJ (2013) The timing of abscission affects dispersal distance in a wind-dispersed tropical tree. *Functional Ecology*, **27**, 208–218. doi: 10.1111/1365-2435.12028.

McVicar TR, Roderick ML (2010) Winds of change. *Nature Geoscience*, **3**, 747–748. doi: 10.1038/ngeo1002.

McVicar TR, Roderick ML, Donohue RJ, Van Niel TG (2012a) Less bluster ahead? Overlooked ecohydrological implications of global trends of terrestrial near-surface wind speeds. *Ecohydrology*, **5**, 381–388. doi: 10.1002/eco.1298.

McVicar TR, Roderick ML, Donohue RJ, et al. (2012b) Global review and synthesis of trends in observed terrestrial near-surface wind speeds: implications for evaporation. *Journal of Hydrology*, **416–417**, 182–205. doi: 10.1016/j.jhydrol.2011.10.024.

McVicar TR, Van Niel TG, Li LT, Roderick ML, Rayner DP, Ricciardulli L, Donohue RJ (2008) Wind speed climatology and trends for Australia, 1975–2006: capturing the stilling phenomenon and comparison with near-surface reanalysis output. *Geophysical Research Letters*, **35**. doi: 10.1029/2008GL03562.

Moles AT, Westoby M (2004) Seedling survival and seed size: a synthesis of the literature. *Journal of Ecology*, **92**, 372–383. doi: 10.1111/j.0022-0477.2004.00884.x.

Nathan R, Horvitz N, He Y, Kuparinen A, Schurr F, Katul G (2011a) Spread of North-American wind-dispersed trees in future environments. *Ecological Letters*, **14**, 211–219. doi: 10.1111/j.1461-0248.2010.01573.x.

Nathan R, Katul GG (2005) Foliage shedding in deciduous forests lifts up long-distance seed dispersal by wind. *Proceedings of the National Academy of Sciences of the United States of America*, **102**, 8251–8256. doi: 10.1073/pnas.0503048102.

Nathan R, Katul GG, Bohrer G, et al. (2011b) Mechanistic models of seed dispersal by wind. *Theoretical Ecology*, **4**, 113–132. doi: 10.1007/s12080-011-0115-3.

Nathan R, Katul GG, Horn HS, et al. (2002) Mechanisms of long-distance dispersal of seeds by wind. *Nature*, **418**, 409–413. doi: 10.1038/nature00844.

Okubo A, Levin SA (1989) A theoretical framework for data analysis of wind dispersal of seeds and pollen. *Ecology*, **70**, 329–338. doi: 10.2307/1937537.

Pazos GE, Greene DF, Katul GG, Bertiller MB, Soons MB (2013) Thresholds for seed abscission in wind dispersal. *Ecology*, In Review.

Poggi D, Katul GG, Albertson J (2006) Scalar dispersion within a model canopy: measurements and three-dimensional Lagrangian models. *Advances in Water Resources*, **29**, 326–335. doi: 10.1016/j.advwatres.2004.12.017.

Portnoy S, Willson MF (1993) Seed dispersal curves: behavior of the tail of the distribution. *Evolutionary Ecology*, **7**, 25–44. doi: 10.1007/BF01237733.

Prandtl L (1904) Motion of fluids with very little viscosity. *3rd International Mathematics Congress*. Wiley, Heidelberg.

Raupach MR, Thom AS (1981) Turbulence in and above plant canopies. *Annual Review of Fluid Mechanics*, **13**, 97–129. doi: 10.1146/annurev.fl.13.010181.000525.

Roderick ML, Rotstayn LD, Farquhar GD, Hobbins MT (2007) On the attribution of changing pan evaporation. *Geophysical Research Letters*, **34**. doi: 10.1111/j.1749-8198.2008.00214.x.

Schippers P, Jongejans E (2005) Release thresholds strongly determine the range of seed dispersal by wind. *Ecological Modelling*, **185**, 93–103. doi: 10.1016/j.ecolmodel.2004.11.018.

Skarpaas O, Auhl R, Shea K (2006) Environmental variability and the initiation of dispersal: turbulence strongly increases seed release. *Proceedings of the Royal Society B-Biological Sciences*, **273**, 751–756. doi: 10.1098/rspb.2005.3366.

Soons MB, Bullock JM (2008) Non-random seed abscission, long-distance wind dispersal and plant migration rates. *Journal of Ecology*, **96**, 581–590. doi: 10.1111/j.1365–2745.2008.01370.x.

Stoy P, Katul G, Siqueira M, et al. (2006) Separating the effects of climate and vegetation on evapotranspiration along a successional chronosequence in the South-Eastern US. *Global Change Biology*, **12**, 2115–2135. doi: 10.1111/j.1365-2486.2006.01244.x.

Sudo S, Matsui N, Tsuyuki K, Tetsuya Y (2008) Morphological design of dandelion. *XIth International Congress and Exposition, Society for Experimental Mechanics*. Society for Experimental Mechanics, Orlando, Florida.

Tackenberg O (2003) Modeling long-distance dispersal of plant diaspores by wind. *Ecological Monographs*, **73**, 173–189.

Thompson SE, Alvarez-Loayza P, Terborgh J, Katul GG (2010) The effects of plant pathogens on tree recruitment in the Western Amazon under a projected future climate: a dynamical systems analysis. *Journal of Ecology*, **98**, 1434–1446. doi: 10.1111/j.1365-2745.2010.01726.

Thompson SE, Katul GG (2008) Plant propagation fronts and wind dispersal: an analytical model to upscale from seconds to decades using superstatistics. *American Naturalist*, **171**, 468–479. doi: 10.1086/528966.

Thompson SE, Katul GG, McMahon SM (2008) Role of biomass spread in vegetation pattern formation within arid ecosystems. *Water Resources Research* **44**, W10421. doi: 10.1029/2008WR006916.

Thompson SE, Katul GG, Terborgh J, Alvarez-Loayza P (2009) Spatial organization of vegetation arising from non-local excitation and local inhibition in tropical rainforests. *Physica D*, **238**, 1061–1067. doi: 10.1016/j.physd.2009.03.004.

Van der Hoven I (1957) Power spectrum of horizontal wind speed in the frequency range from 0.0007 to 900 cycles per hour. *Journal of Meteorology*, **14**, 160–164.

Vautard R, Cattiaux J, Yiou P, Thepaut JN, Ciais P (2010) Northern Hemisphere atmospheric stilling partly attributed to an increase in surface roughness. *Nature Geoscience*, **3**, 756–761. doi: 10.1038/ngeo979.

Wei G, Shalei S, Bo Z, Shuo S, Faquan L, Xuewu C (2012) Multi-wavelength canopy lidar for remote sensing of vegetation: design and system performance. *ISPRS Journal of Photogrammetry and Remote Sensing*, **69**, 1–9.

Westoby M, Jurado E, Leishman M (1992) Comparative evolutionary ecology of seed size. *Trends in Ecology and Evolution*, **7**, 368–372. doi: 10.1016/0169-5347(92)90006-W.

Wilson JD (2000) Trajectory models for heavy particles in atmospheric turbulence: comparison with observations. *Journal of Applied Meteorology*, **39**, 1894–1912. doi: 10.1175/1520-0450.

Wright SJ, Trakhtenbrot A, Bohrer G, et al (2008) Understanding strategies for seed dispersal by wind under contrasting atmospheric conditions. *Proceedings of the National Academy of Sciences*, **105**, 19084–19089. doi: 10.1073/pnas.0802697105.

Xu M, Chang CP, Fu C, Qi Y, Robock A, Robinson D, Zhang H (2006) Steady decline of east Asian monsoon wind speed. *Journal of Geophyiscal Research*, **111**. doi: 10.1029/2006JD007337.

Supporting Information

Additional Supporting Information may be found in the online version of this article:

Data S1: The effect of non-Gaussian u' distributions on the functional form of $f(u)$ and $g(u^*)$ Data S2: A detailed outline of the tree sway or 'beam deflection' model, including its nondimensionalization Data S3: The full equations for the IP-CELC model Data S4: The source and illustration of the wind statistics distributions used for the Eulerian component of IP-CELC Data S5: Description of the WALD model and the maximum likelihood approach to determining its parameters.